Supplementary Materials

a

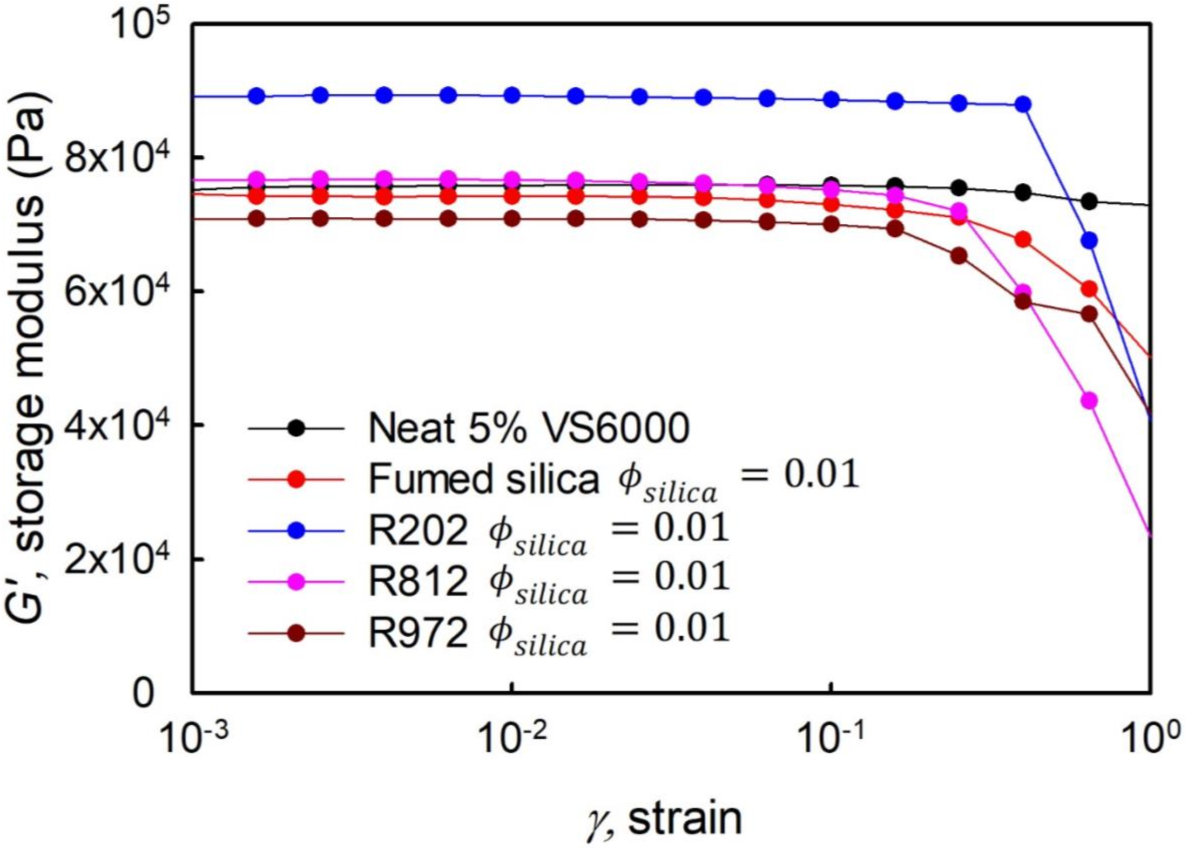

b

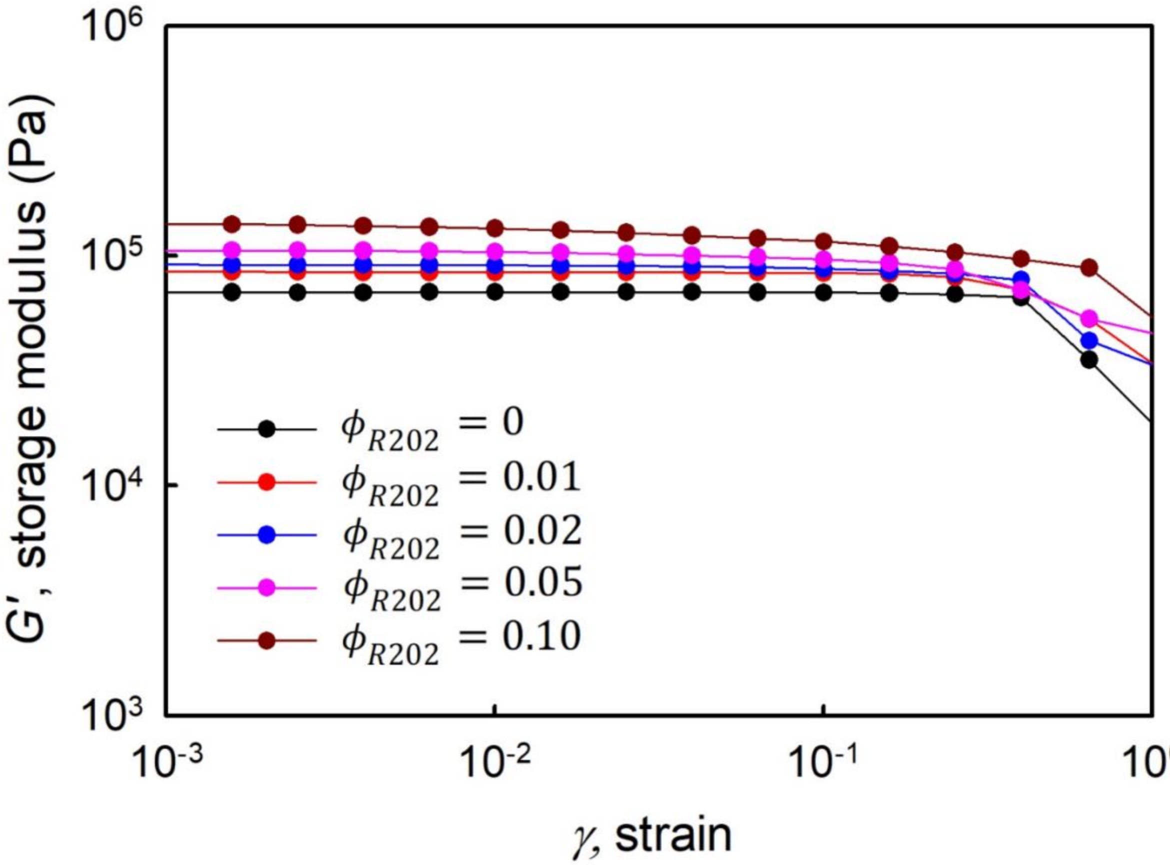

Figure S1. Comparison of the rheological properties of silica filled silicone nanocomposites. a) Strain sweep of the silicone containing different silica as nanofillers. b) Strain sweep of R202 filled silicone nanocomposite with different ϕ_{R202}.

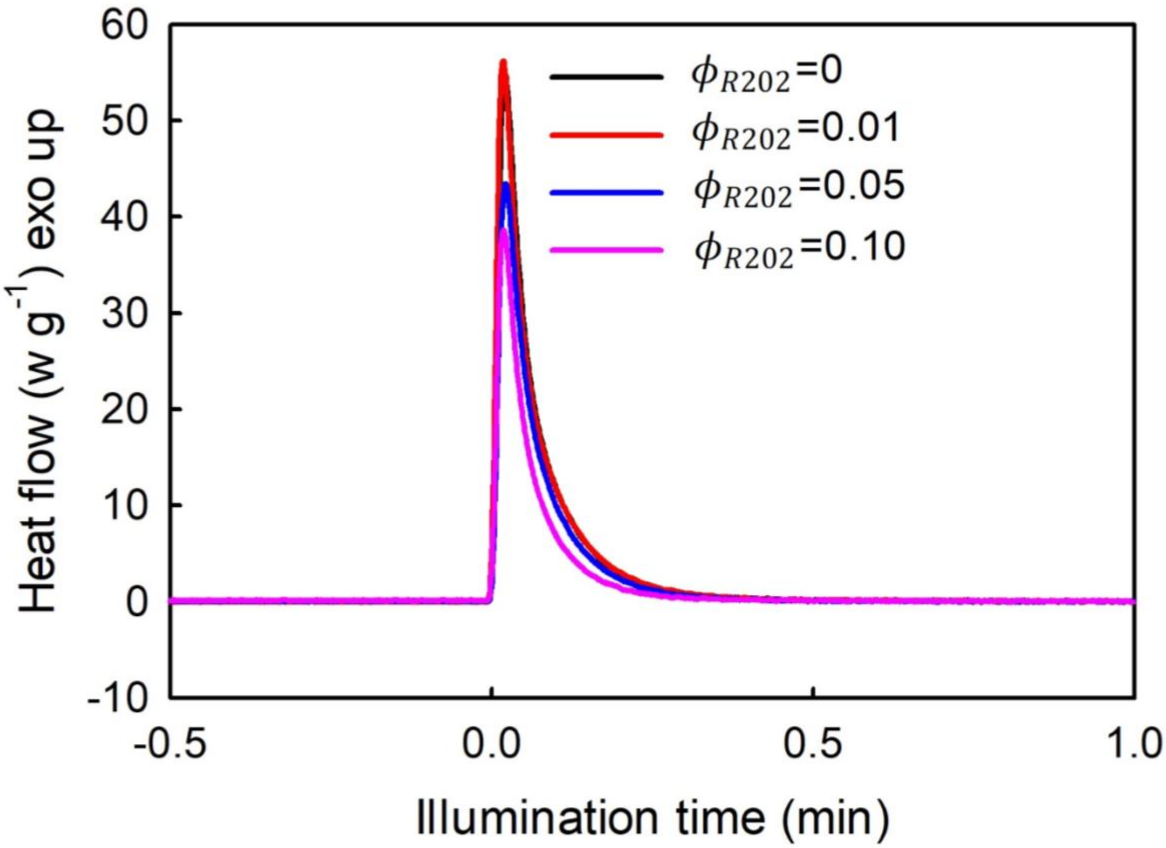

Figure S2. Photo-DSC of the R202 silica-silicone pre-gel suspensions, in comparison to the neat 5% VS6000 pre-gel solution ($\phi_{R202} = 0$).

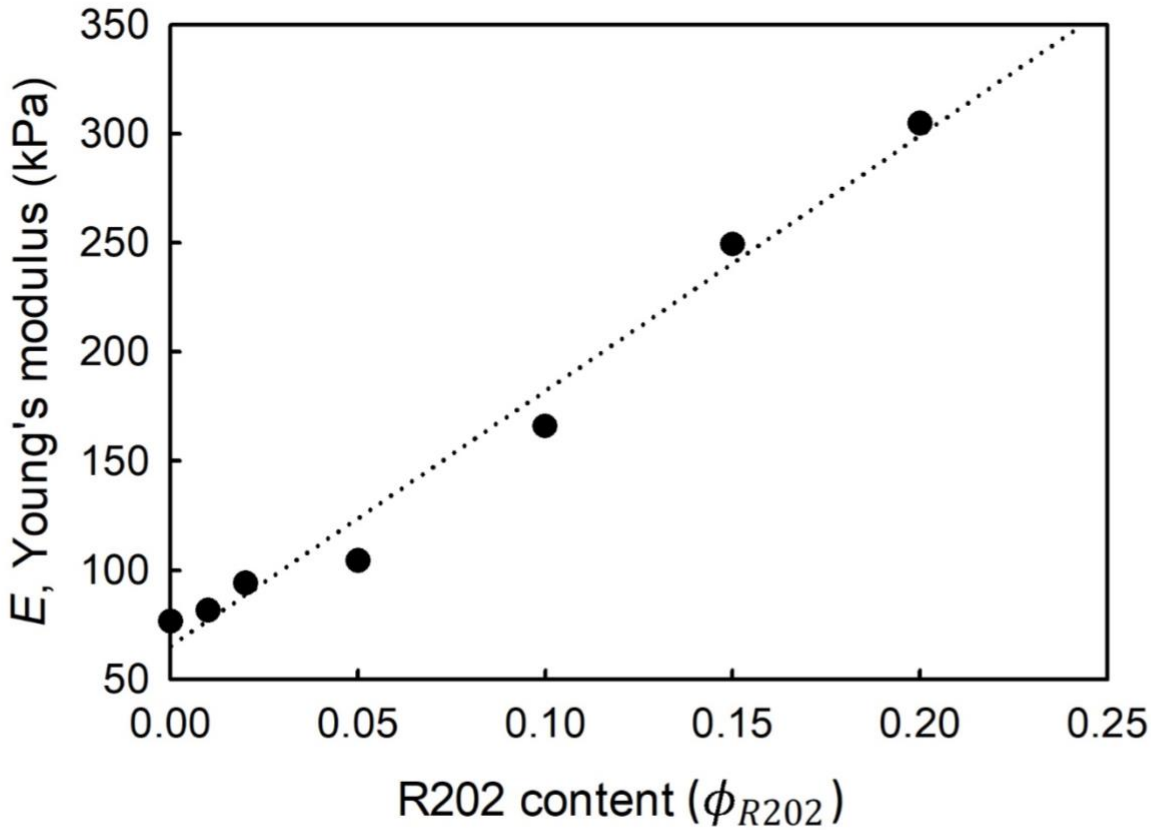

Figure S3. Tangent modulus (*E*) vs. R202 content (ϕ_{R202}).

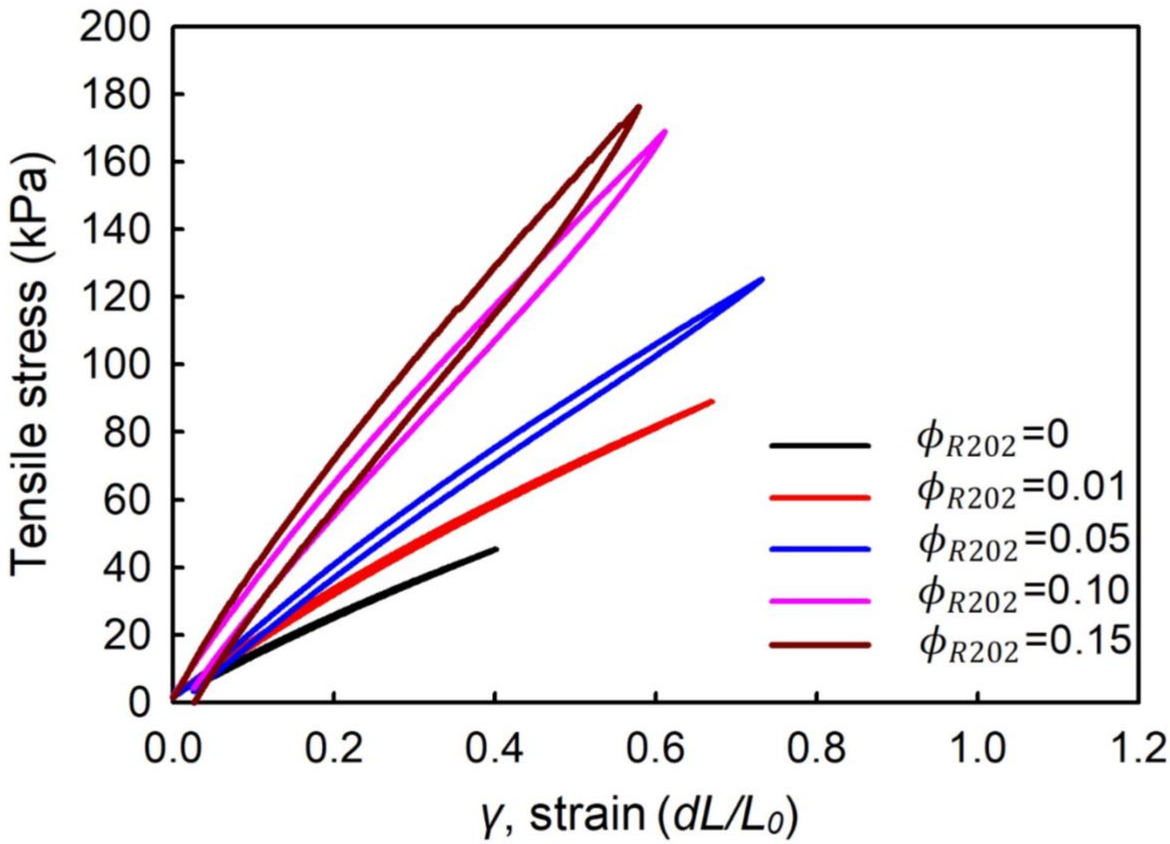

Figure S4 Cycle 0 (training cycle) of R202 filled silicone, from cyclic tensile tests.

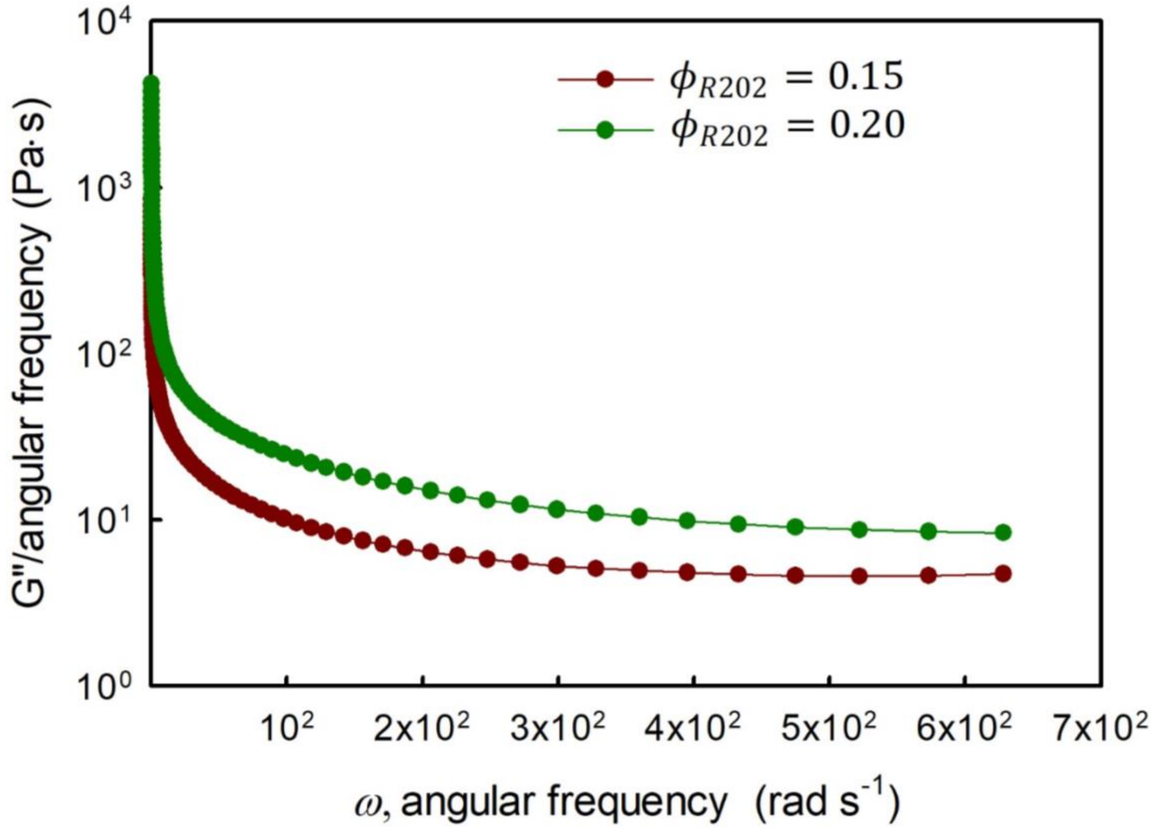

Figure S5. Angular frequency vs. G"/angular frequency, of silica-silicone suspensions (ϕ_{R202} = 0.15 and 0.20).

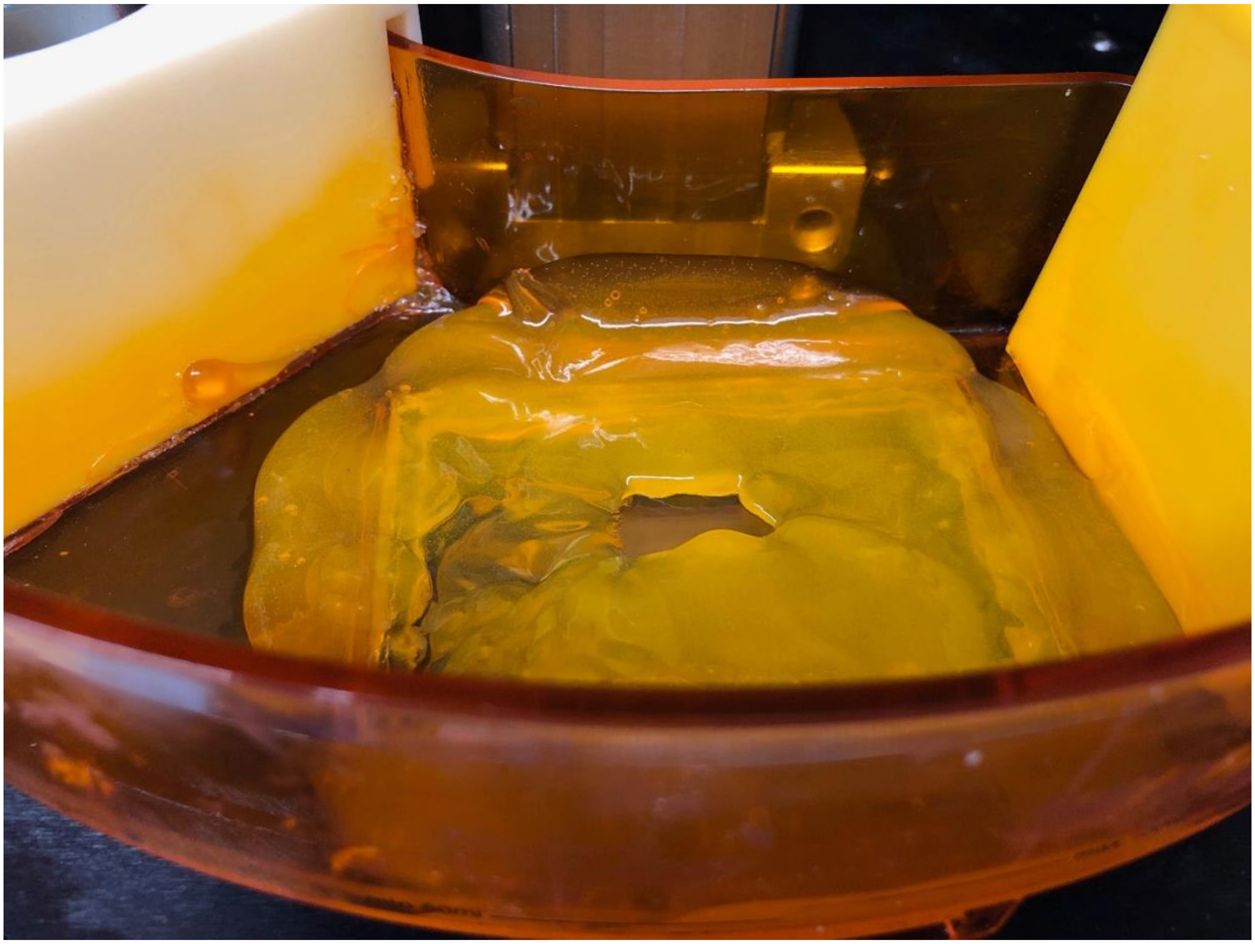

Figure S6. The void, which is left on the window when printing ϕ_{R202} = 0.20 suspensions due to sluggish recoating, eventually leads to printing failure.

a

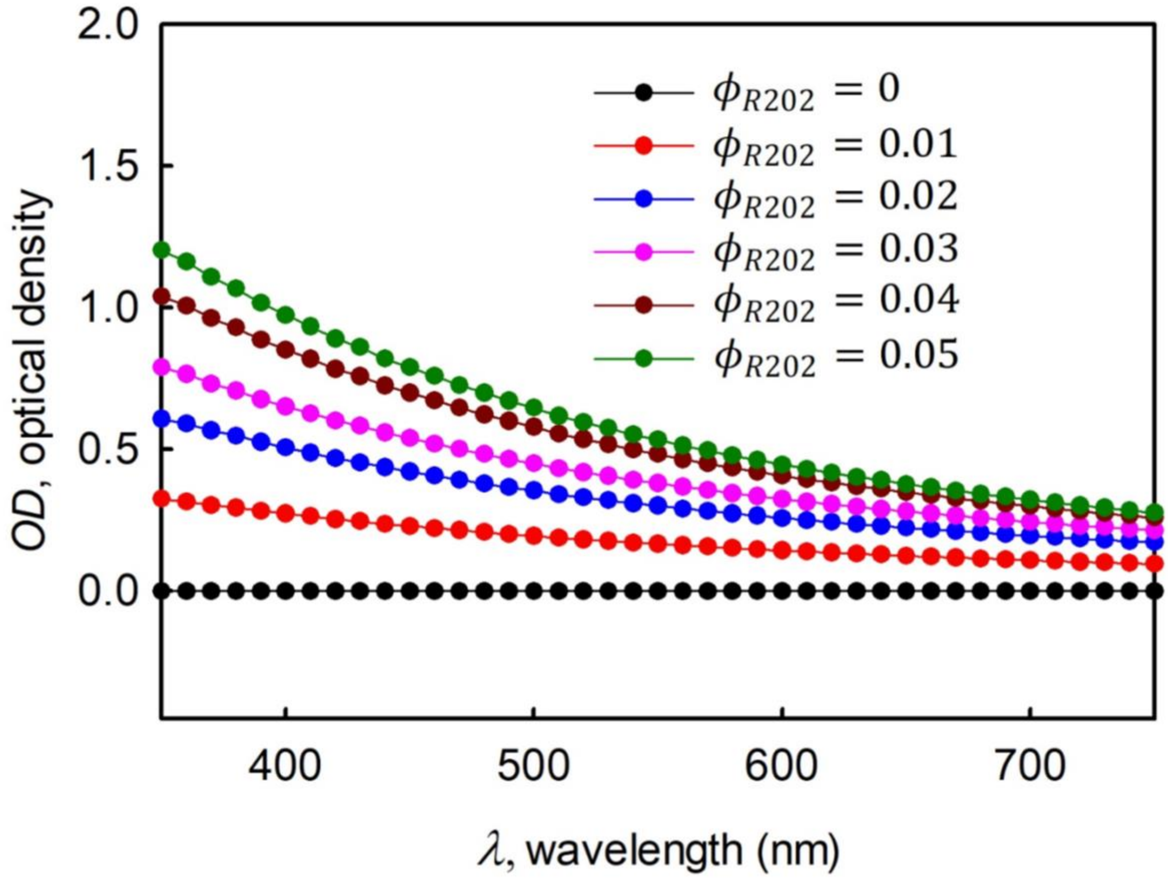

2.0
1.5
1.0
0.5
0.0
400
500
600
700
OD, optical density
λ, wavelength (nm)
$\phi_{R202} = 0$
$\phi_{R202} = 0.01$
$\phi_{R202} = 0.02$
$\phi_{R202} = 0.03$
$\phi_{R202} = 0.04$
$\phi_{R202} = 0.05$

b

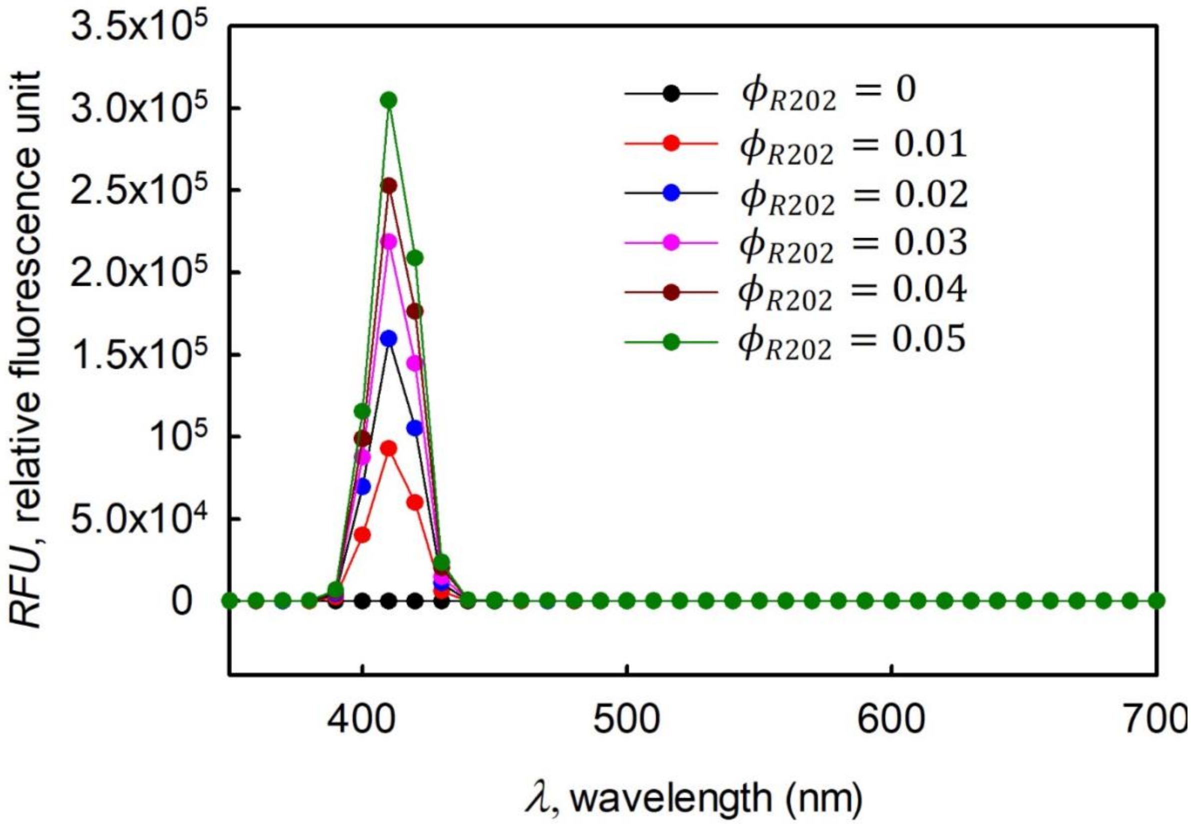

Figure S7. a) Absorption spectra of the silica-silicone suspensions from 300 to 750 nm; b) Emission spectra of the silica-silicone suspensions collected from 350 to 700 nm, when excited by 410 nm light.

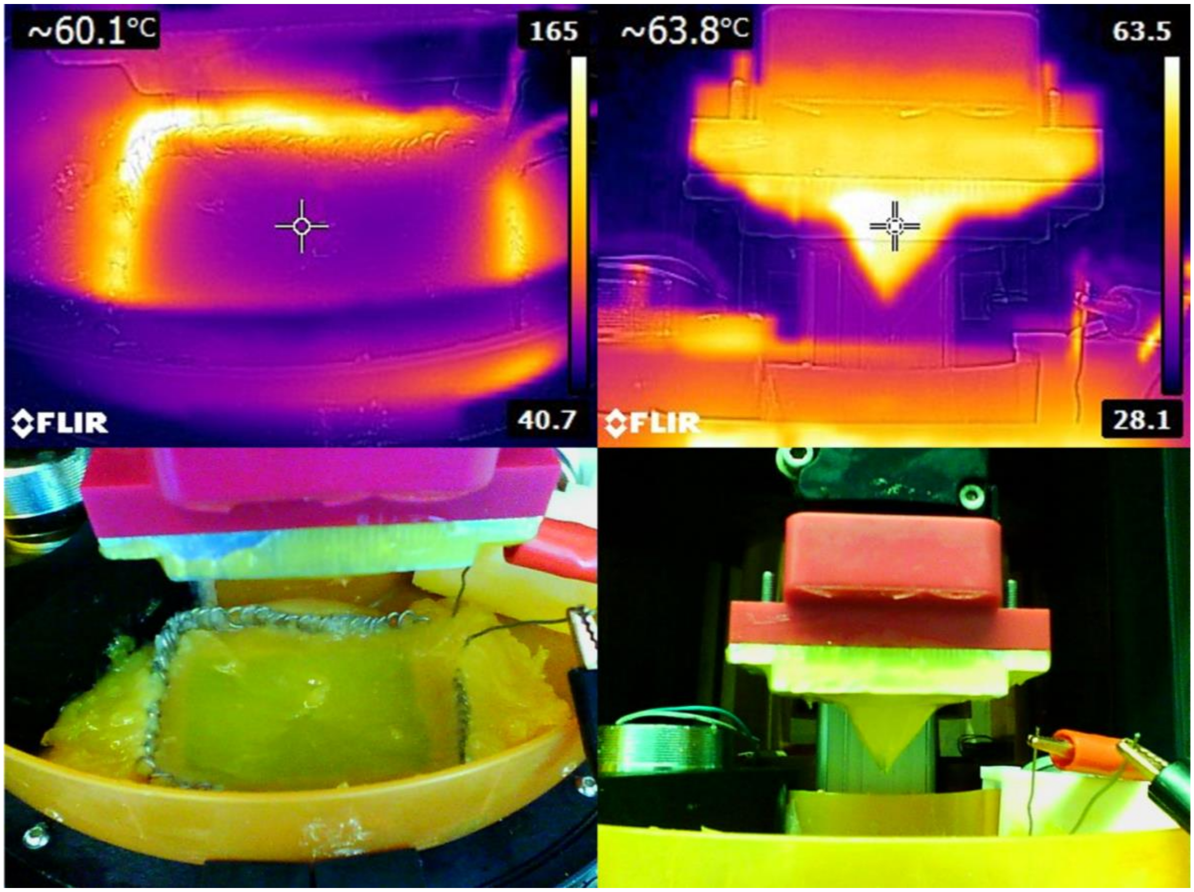

Figure S8. Heat-assisted printing. The images taken by thermal camera show that the central part of the tray is maintained at 60 ℃ during printing.

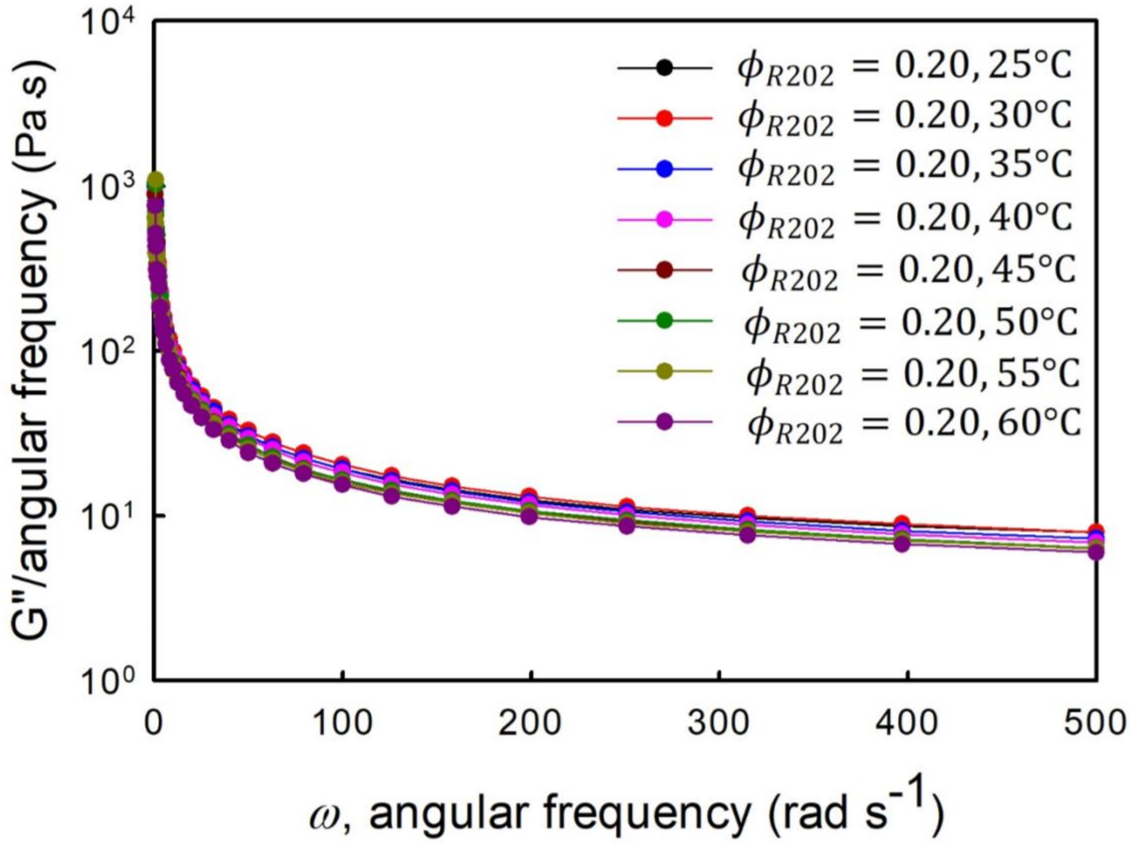

Figure S9. Angular frequency vs. G"/angular frequency, of silica-silicone suspensions (ϕ_{R202} = 0.20) at different temperatures.

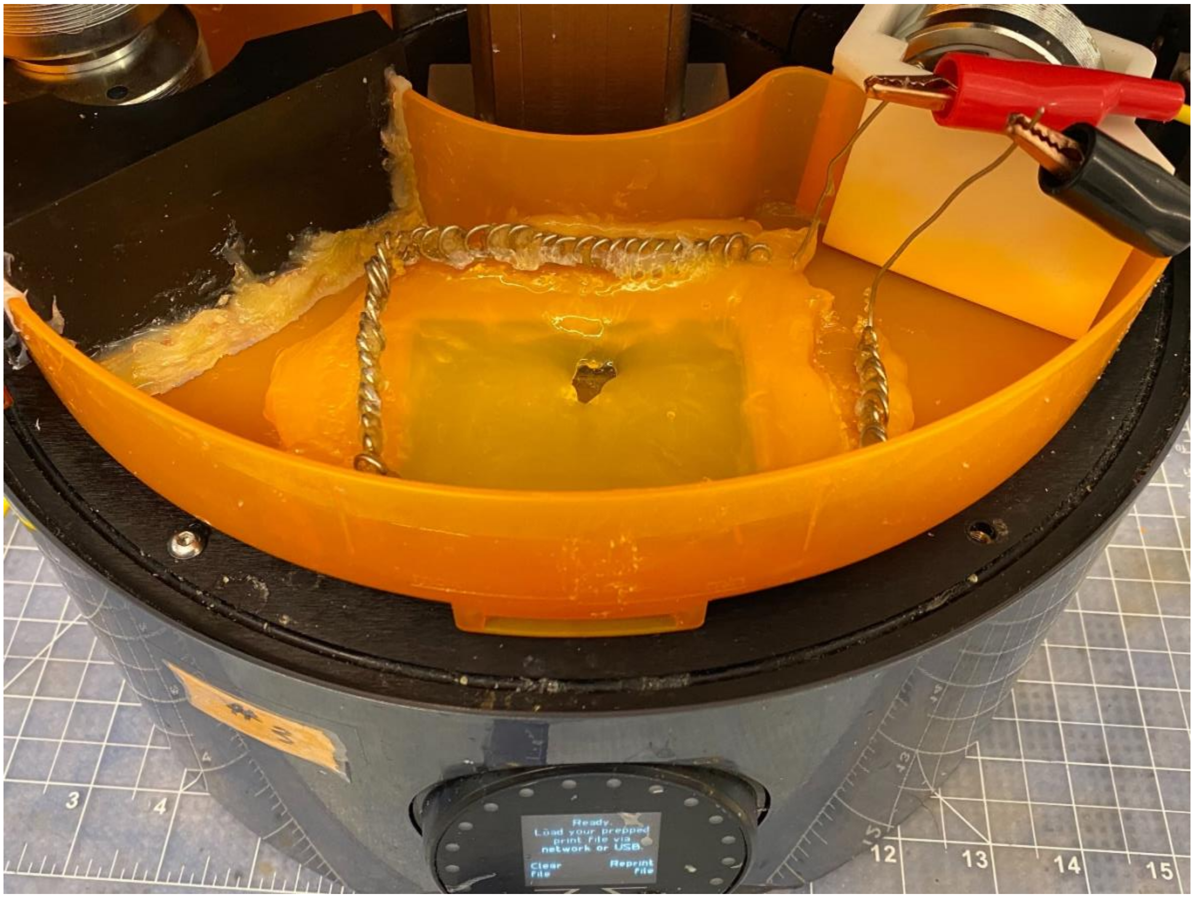

Figure S10. Print failure of ϕ_{R202} = 0.20 suspensions at 60 ℃ with build-head speed setting at 1 mm/s.

Calculation of Relaxation Time τ_p

The linear viscoelastic properties of hard-sphere suspensions can be measured by the characteristic particle relaxation time, τ_p, which corresponds to how long the suspensions can relax their interparticle spacings [1-2].

$$\tau_p(\phi) = \frac{\pi \eta'_\infty(\phi) a^3}{k_B T}$$

where *a* is the radius of particle, *T* is temperature, k_B is Boltzmann constant and $\eta'_\infty(\phi)$ is high frequency viscosity. For suspension with a particle content ϕ, its high frequency viscosity is expected to be approaching to a constant value. $\eta'_\infty(\phi)$ is defined as

$$\eta'_\infty(\phi) = \lim_{\omega \to \infty} \frac{G"(\phi)}{\omega}$$

where *G*" is the loss modulus and ω is the angular frequency. We plotted G"/ω against ω for ϕ = 0.15 and 0.20. (Fig. S5) From the plot, we can further deduce $\eta'_\infty(0.15)$ = 4 Pa·s and $\eta'_\infty(0.20)$ = 7 Pa·s. We assume *a* = 20 nm and T = 298.15 K, therefore, $\tau_p(0.15)$ and $\tau_p(0.20)$ are 0.02 s and 0.05 s, respectively.

Estimation of hydrostatic pressure in the recoating process of top-down SLA

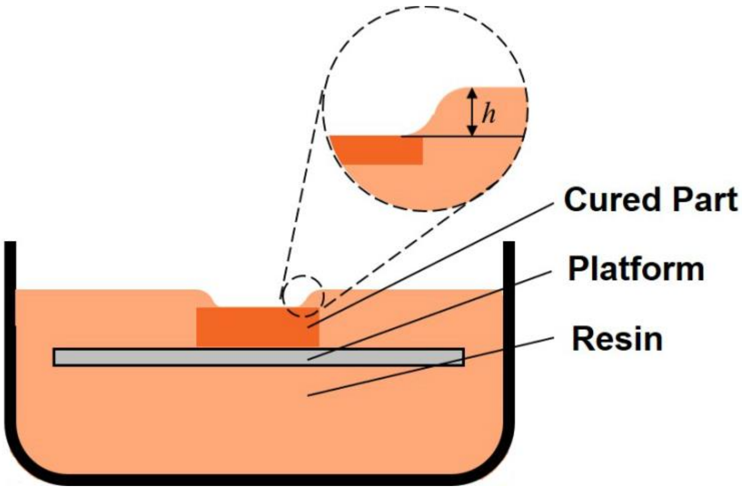

A schematic plot showing the profile of resin surface after the flatform is moved down for one layer thickness *h*.

As shown in the figure above, the hydrostatic pressure caused by gravity can be estimated as

$$P = \rho \cdot g \cdot h$$

where h is layer thickness, ρ is resin density, and g is the gravity of earth.
If we assume the layer thickness h = 100 µm, and the density ρ~1 g·cm^{-3}; we can get P~1 Pa.

References

[1] R. G. Larson, *The structure and rheology of complex fluids*, Vol. 150, Oxford university press New York, 1999.
[2] T. Shikata, D. S. Pearson, Journal of Rheology 1994, 38, 601.